

Kinetics of differentiated stylolite formation

S. Sinha-Roy

Birla Institute of Scientific Research, Statue Circle, Jaipur 302 001, India

Stylolites are discontinuity structures in rocks, and are represented by seams of insoluble residues in partings. These are the products of pressure solution attending diagenetic compaction and post-diagenetic deformation of sediments. There are several problems concerning the genesis of stylolites, especially of those showing differentiated geometry such as conical, columnar and wavy types of mutual interdigitations between rock-block partners. These problems have been addressed here on the basis of the study of stylolites developed in limestones of the Lower Vindhyan sequence, SE Rajasthan. A kinetic model has been proposed for the formation and differentiation of stylolites. This involves pressure solution mechanism, textural instability in the rock, fluid-flow polarity changes, fluid-flow perturbations, and progressive diagenetic and/or tectonic strain and its local partitioning.

STYLOLITES are generally considered as diagenetic and/or post-diagenetic tectonic structures developed in sedimentary rocks, particularly in limestones, and are represented by partings of insoluble residues between blocks of rock mass that exhibit complex mutual interdigitations. The geometry of stylolite is variable from planar, conical, columnar and wavy types, depending on the shape of the stylolite seams in 2D. Generally, the stylolites are initiated¹ as discontinuous, discrete and smooth pressure solution seams (planar type), which progressively change into conical, columnar and wavy types. The type of stylolite that shows conical, columnar and wavy profiles is designated as the differentiated stylolite. The mechanism of formation of stylolites in general, and of the differentiated type in particular, is problematic.

Many studies on stylolites and pressure solution structures have revealed that their origins are controversial. Among the various mechanisms suggested¹, pressure solution is generally accepted as the most likely mechanism of stylolite genesis². In spite of, and perhaps because of this, there exist a number of problems concerning stylolite genesis. The most important among these are the following.

(a) Stylolites are secondary structural and textural discontinuities in a rock mass. The controls of such discontinuities and the reasons for the initial stylolites being

located at a given site are not clearly known. Some workers suggested that pressure solution at selected sites in the rock mass involves nonlinear physico-chemical processes such as pore-fluid pressure, temperature, burial rate of sediments, rock textures, etc.³. It has also been suggested that early joints and microfractures can be reactivated as stylolite during later deformation and associated pressure solution⁴. The initial planar stylolite seams are also viewed as 'anticracks', their lateral propagation considered similar to that of tensile cracks⁵.

(b) It has been suggested⁶ that stylolites develop under stress at sites of textural heterogeneity caused by uneven distribution of mineral grains of variable pressure solubility. The problem in this case is related to the kinetics of 'planar' stylolite formation in a rock mass of inhomogeneous texture and mineralogy showing 'punctual' heterogeneity².

(c) The kinetics of rock response to overall applied stress, by generating within itself regions of high and low solubility, one of the controlling factors of stylolite genesis, is problematic.

(d) Somewhat related to point (c) above is the problem of stylolite differentiation and the amplification of the interdigitations. The explanations given by different workers for the differentiated stylolite geometry are variable. These are: (i) differential pressure solubility of the rock-block partners and of the mineral grain pairs parallel to the maximum compressive stress direction⁶, (ii) polarity reversal of the solvent fluid migration^{7,8}, and (iii) the natural instability of the rock mass created by the differential porosity-permeability regimes⁸.

Any explanation for the geometry and genesis of stylolites must necessarily take these problems into consideration.

The above problematic aspects related to the kinetics of stylolite genesis make the differentiated stylolites a complex and little-understood structural feature in sedimentary rocks. The purpose of this communication is to address some of these problems, and to propose a kinetic model for the origin and amplification of differentiated stylolites. The model is based on the study of the stylolites, particularly their microstructures, developed in the Nimbahera Limestone of the Semri Group, Lower Vindhyan Supergroup, in Nimbahera area, SE Rajasthan.

The definition of some of the terms concerning the stylolite geometry used here is as follows. The different elements of a hypothetical differentiated stylolite developed under the influence of triaxial compaction stress system ($\sigma_1 > \sigma_2 > \sigma_3$) are shown in Figure 1. The *stylolite seam* (SS) is the parting consisting of insoluble residues, generally opaque and clay minerals, between the two rock-block partners (X, Y). Generally, the seam differentiation is discernible in one profile parallel to

e-mail: ssinharoy@yahoo.com

$\sigma_1 - \sigma_2$ plane, but intersecting sets of stylolite developed on nearly orthogonal planes⁷, and interdigitations of the same stylolite seam on profiles parallel to both $\sigma_1 - \sigma_2$ and $\sigma_1 - \sigma_3$ planes⁹, are not uncommon. The latter types are complex stylolites developed in a stress regime usually during sediment compaction and diagenesis followed by tectonic deformation, where σ_1 and σ_2 may locally swap positions.

In order to describe the stylolite morphology and microstructures, the following structural elements are considered. The *stylolite plane* (SP) is the planar part or the enveloping surface of differentiated stylolite which is oriented perpendicular to σ_1 . The SP is generally the initial pressure solution surface that progressively differentiates. In 2D on $\sigma_1 - \sigma_2$ profile the differentiated stylolite seam has conical, columnar and wavy shapes. In 3D, however, the forms are simple prismatic for the conical type, tetrahedral prismatic for the columnar type, and cylindrical for the wavy type. The *stylolite axis* (SA) is the hinge-line of the prism parallel to the lines of intersection of the sides of the prism, and to the cylinder axis. The SA geometry is similar to that of fold structures. The stylolite geometry will henceforth be considered in 2D here. The *stylolite head* (SH) is the apical region of the conical, columnar and wavy types, while the *stylolite limbs* (SL) are their sides. The *stylolite axial plane trace* (SAP) is the line bisecting the interlimb angle of the cones, columns and wavy types. The *stylolite facing* (F) is the direction pointed by the apexes of the cones and columns. The stylolite is considered symmetric if the facing is perpendicular to the stylolite plane and parallel to σ_1 , and asymmetric if the facing is oblique to the stylolite plane.

The host rock of the studied stylolites is pink-to-grey, well-cemented limestone which contains siliceous and argillaceous bands and partings of variable thickness. The groundmass consists of fine to very fine-grained

calcite, and a few quartz, microscopically unresolvable clay and dispersed opaque mineral grains. Small patches (30–100 μm) of sparry calcite occur in the host-rock, mostly away from the stylolite zone.

The stylolites developed in the Lower Vindhyan limestones of SE Rajasthan have been studied in hand specimens and under the microscope. The geometry and microstructures of these stylolites are variable^{9,10}. The stylolite plane is generally parallel or at a low angle (10–15°) to the bedding plane of the limestone. The planar or nearly-planar type of stylolite is rare, but wherever such a type occurs, it is thin (30–50 μm wide), and wedge-shaped. The differentiated stylolites are generally wavy and columnar types in which the width of the head (70–120 μm) is invariably greater than that of the limbs (15–50 μm). The wavy type has a sinusoidal profile and maintains almost uniform thickness at the limb and head regions and thus resembles flexural folds, although not originating from layer-parallel shortening. Generally, the stylolite axes are unstable so that in 3D the stylolite geometry is variable. The conical type is mostly associated with nearly planar to gently corrugated stylolite seams (Figure 2) that are thinner than the seams defining the columnar and wavy types. The amplitude and the wavelength of the conical type are lower than those of the columnar and wavy types. The amplitude of the columnar type is greater by an order of 1.5 to 2.5 than that of the wavy type, and the wavelength of the wavy type is greater than that of the columnar type. Notably, the concentration of the opaque minerals in the conical head segments is much higher than that in the planar limb segments of the same stylolite zone (Figure 2). This feature suggests that the frequency and the distribution pattern of the opaque mineral grains in the matrix play an important role in the differentiation of stylolites.

Many stylolite seams are lined with discontinuous mineral bands (20–600 μm wide) composed of fibres of dominantly calcite, minor quartz and chlorite (Figure 3). These mineral bands, termed as ‘fibrous bands’¹⁰, generally show antitaxial fibre growth kinetics. Calcite and quartz have precipitated in these bands from the saturated fluid that pressure-dissolved the limestone at the stylolite seam¹⁰. Fibres show a preferred dimensional orientation nearly parallel to the stylolite axial plane trace and the stylolite facing, but are generally orthogonal to the stylolite plane. Assuming that the stylolite axial plane is parallel to σ_1 and the stylolite plane is perpendicular to σ_1 , the fibre long-axis gives the orientation of the local and instantaneous σ_1 axis.

The stylolite seam material consists of opaque minerals (goethite, pyrite), diagenetic clay minerals (dominantly illite), and minor amounts of chlorite and glauconite. XRD analysis indicated the presence of minor quantities of calcite and quartz within the stylolites seams. These are either residual host-rock compo-

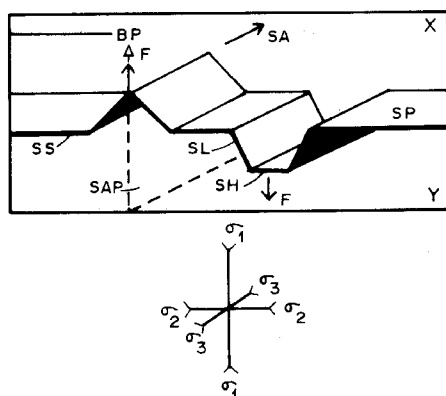


Figure 1. Profile of hypothetical differentiated stylolite showing the different stylolite elements and their relations with the stress system ($\sigma_1 > \sigma_2 > \sigma_3$). BP, Bedding plane; F, Stylolite facing; SA, Stylolite axis; SAP, Stylolite axial plane; SH, Stylolite head; SL, Stylolite limb; SP, Stylolite plane; SS, Stylolite seam.

nents that are not pressure-dissolved because of the supersaturation of the fluid or they represent the mineral phases precipitated from this fluid. The domainal distribution of the stylolite seam minerals defines a secondary compositional layering within the stylolite seams. This layering is either planar (Figure 3) or kinked (Figure 4). The planar layering at the two ends of some stylolite heads is dragged inside the corresponding inclined limbs along the shear planes bounding such limbs (Figure 3). These limb-shears may extend inside the stylolite head, offsetting the stylolite seam. The end segments of the head that are inclined at a low-to-moderate angle to the stylolite plane show kink-bands on the secondary compositional layering. The kink-planes on the inclined head are parallel to the adjacent limb segment where the stylolite seam is attenuated and boudinaged. The boudins are rotated due to resolved shear strain on the limbs (Figure 4). In the steeply inclined limb segments where the limbs make 70–80° angle with the stylolite plane, extremely thin (10–20 µm) stylolite seams show nearly symmetric buckle folds with the axial plane trace nearly parallel to the corresponding stylolite plane trace. This microstructure is interpreted as having developed due to initial stretching and later folding of the attenuated limb that rotated with respect to the stylolite axial plane from the extensional domain to the shortening domain. Where they are

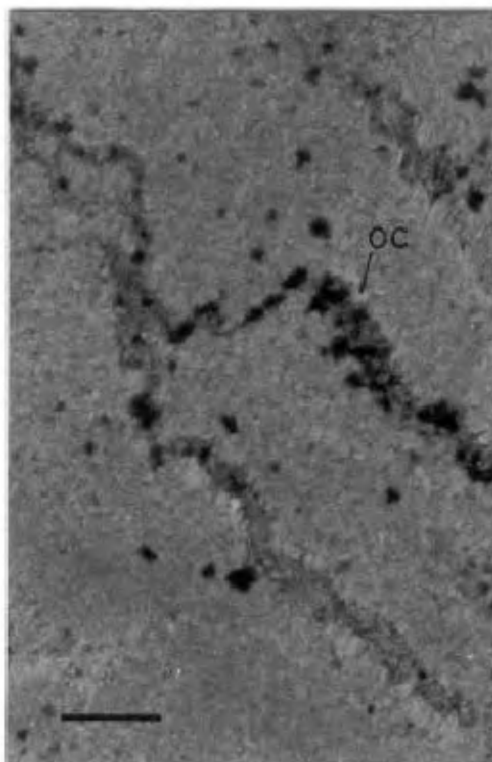


Figure 2. Photomicrograph of planar and conical stylolite (dark bands) developed in fine-grained limestone (grey). Note the preferred stylolite differentiation into cones at or near the sites of opaque mineral clumps (OC). (Scale bar = 0.1 mm).

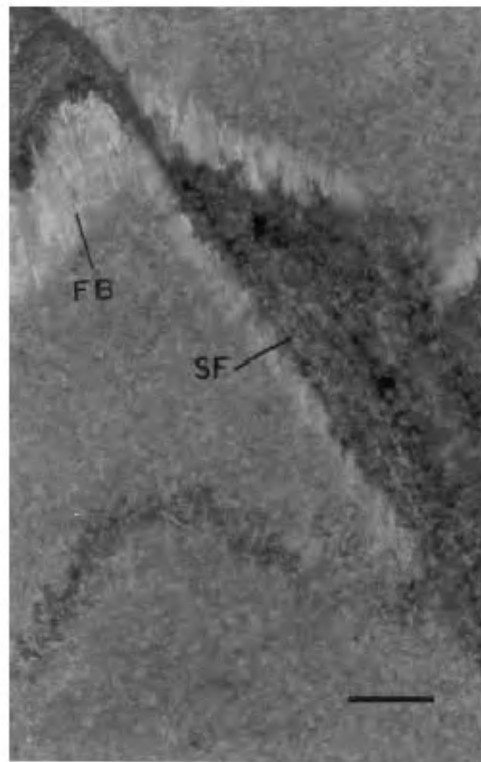


Figure 3. Photomicrograph of a part of wavy stylolite showing planar secondary compositional layering within the stylolite seam (black), fibrous bands (FB) at the seam margins, and displacement of the stylolite seam along a shear fracture (limb-shear) (SF) that has dragged the layers into parallelism with the shear plane in the upper part of the photograph. Note the preferred dimensional orientation of the calcite fibres within the fibrous bands with the fibre axis almost parallel to the stylolite axial plane trace, but oblique to the shear fracture. (Scale bar = 0.1 mm).

inclined at 60–70° to the stylolite plane, the limbs at places show asymmetric folds, indicating a sense of non-coaxial strain consistent with that of boudin rotation and oblique orientation of the internal layering of the stylolite seam with respect to the limb-shears.

Most of the stylolites contain thin (30–50 µm) fractures filled with principally quartz and minor amount of calcite in their vicinity. These fractures are connected with the stylolite seams, and they extend to variable distances away from the seams into the host-rock. From the displacement of the host-rock fabric and of the stylolite elements against these fractures, these are considered shear fractures that are coeval with or post-dated the stylolites. They show a conjugate geometry with the dihedral angle between 40 and 75° (Figure 5). The stylolite axial plane trace generally bisects the dihedral angle, and the stylolite facing is parallel to the acute bisectrix. The internal secondary compositional layering as well as the seam-wall segments of the stylolite limbs, caught between two shear fractures, show sinusoidal curvature indicating a sinistral sense of movement in these zones (Figure 5). Several limb segments, bounded by limb-shears, show curved internal

layers that are roughly asymptotic to the seam margins. These microstructures resemble S-C fabric of non-coaxial strain.

Generally, one of the two sets of shear fractures is better developed than the other, but where both the sets are equally developed their intersections define triangular and rhombic domains at the head regions of conical and wavy stylolite seams. These domains show variable degrees of dissolution, amplifying the apical regions of the stylolite cones. The shear plane intersections seem to act as stylolite head attractors (SHA) (Figure 5). The SHAs may modify the shape of the wavy stylolite from gently curved type to sharply curved type. Although calcite and quartz form the sealing material of these shear fractures, a few thinner fracture zones contain insoluble residues of opaque and clay minerals, suggesting some amount of dissolution of the host-rock in these zones. Since these fractures are connected with the stylolite seams that are the sites of pressure solution, the source of the sealing material is considered the saturated to partially saturated fluid derived from these sites. Some shear fractures are connected with the sparry calcite patches in the host-rock, indicating that the carbonate cementing material of the rock was derived at least partially from the stylolite zones. The width of the sealed shear fractures is variable along the

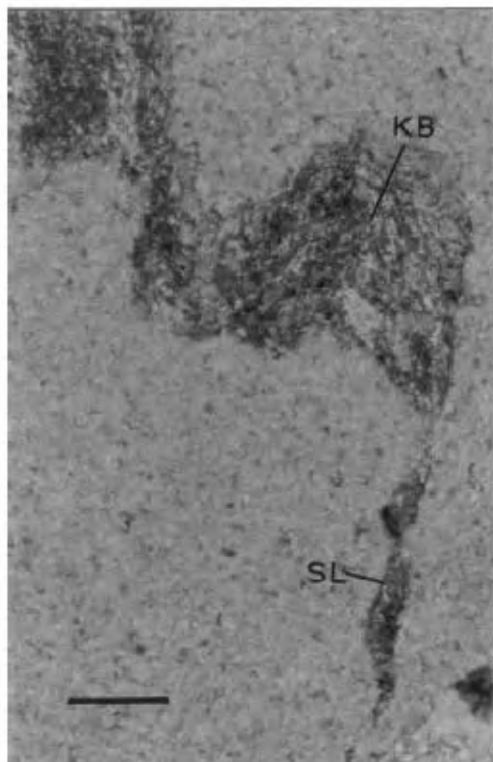


Figure 4. Photomicrograph of a segment of columnar stylolite showing the kink bands (KB) on the secondary compositional layering in the head region of the stylolite seam and the boudinaged nature of the stylolite limb (SL). (Scale bar = 0.1 mm).

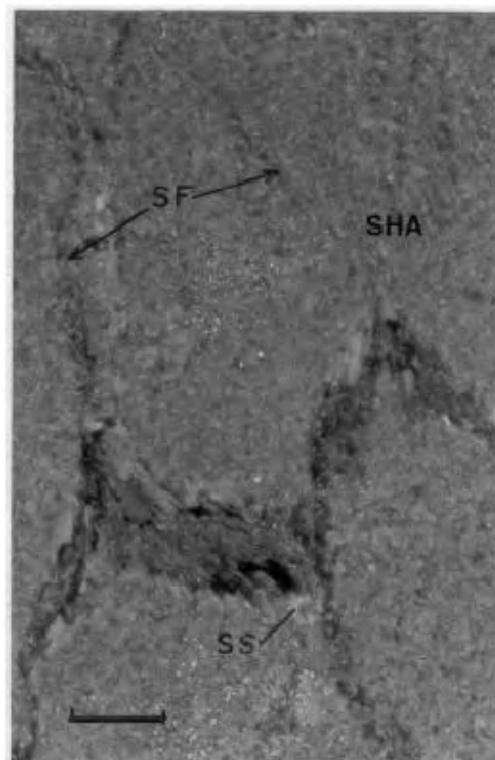


Figure 5. Photomicrograph showing conical stylolite seam (SS) associated with conjugate shear fractures (SF) connected to the apex parts of the cones. Shear fracture intersections acted as stylolite head attractors. Note the continuity of the shear fractures in the stylolite limbs and dextral rotation of a seam segment between two limb-shear planes. (Scale bar = 0.1 mm).

length of the fractures (Figure 6), and some of these contain lens-shaped sealing material composed of fibrous to elongate blocky quartz and calcite grains (Figure 7). The long axes of these fibrous and elongate grains are inclined at 20–40° to the fracture walls. These lenses are interpreted as shear-related pull-apart structures. These calcite and quartz fibres are unrelated to those constituting the fibrous bands around the stylolite seam because the former are syntectonic with respect to shearing, while the fibrous bands are generally pre-shearing in origin¹⁰. Any particular shear plane that displaces both the stylolite seam and the associated fibrous bands, may contain syntectonically-precipitated calcite and quartz fibres (Figure 8a).

From the geometry and microstructures of the stylolites described above, a tentative time-relationship between the different elements can be ascertained. The differentiated stylolites originated from an initially planar and smooth stylolite seam, and the differentiation sequence is from conical to columnar types, the wavy type being a later variant of either of these two types. The shear fracturing of the host-rock is synchronous with stylolite differentiation, but non-coaxial strain outlasted the stylolite and fibrous band development, modifying at places the stylolite geometry. Although

most of the shear fractures are conjugate in nature, mutual displacement and truncation relations (Figure 8b) indicate that shearing in one direction was more prominent than in the other conjugate direction. The fibrous mineral growth within the antitaxial fibrous bands is pre-to-syntectonic in relation to shearing.

The kinetics of stylolite genesis is not fully understood² because of the complex nature of and generally ill-defined relationships that exist between pressure solution mechanism, textural instabilities in the rock, fluid-flow dynamics, and precipitation characteristics of the constituent minerals from the saturated to supersaturated fluids. The geometry and microstructures of stylolites provide important clues to the processes that are involved in stylolite genesis, which depend heavily on the above parameters. It is evident that for the stylolite to originate, two basic conditions must be fulfilled. One is that a stress system must operate on the rock mass, and the other is that inherent textural inhomogeneities must exist in the rock mass. These two factors are explored in a 2D kinetic model proposed here for the genesis of stylolites, especially to explain the little understood mechanism of stylolite differentiation and amplification (Figure 9).

The stress system ($\sigma_1 > \sigma_2 > \sigma_3$) is related to the burial (lithostatic) and the diagenetic compaction of the

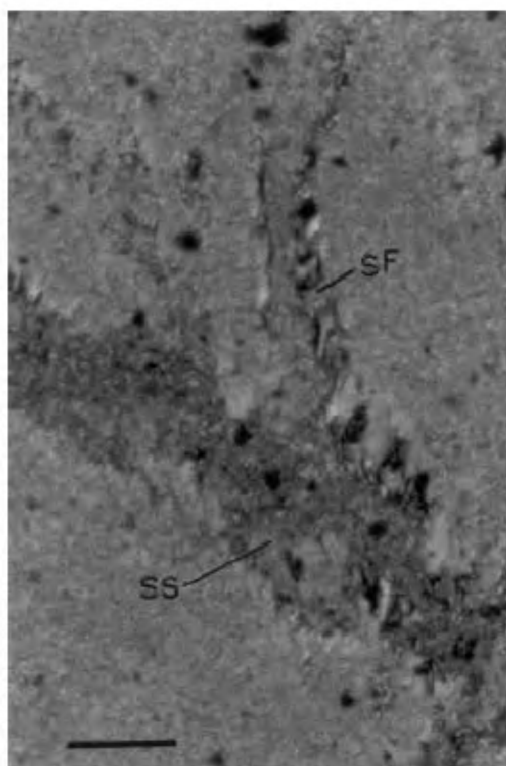


Figure 6. Photomicrograph of stylolite seam (SS) from which a curvilinear and tapering shear fracture (SF) filled with fibrous quartz and calcite extends obliquely into the host-rock. Fibre orientation oblique to the shear fracture walls indicates sinistral sense of movement in the shear fracture zone. (Scale bar = 0.1 mm).

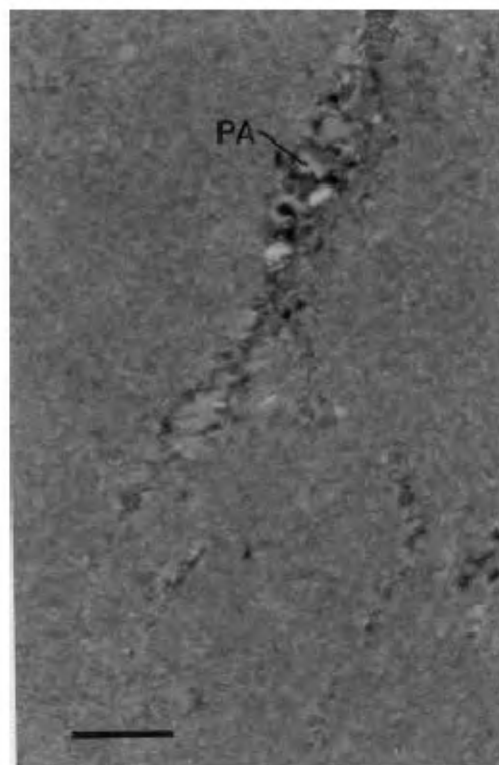


Figure 7. Photomicrograph showing part of a sealed shear fracture containing 'pull-apart' zone (PA) filled with dominant quartz and minor calcite. Note the conjugate orientation of the shear fractures. (Scale bar = 0.1 mm).

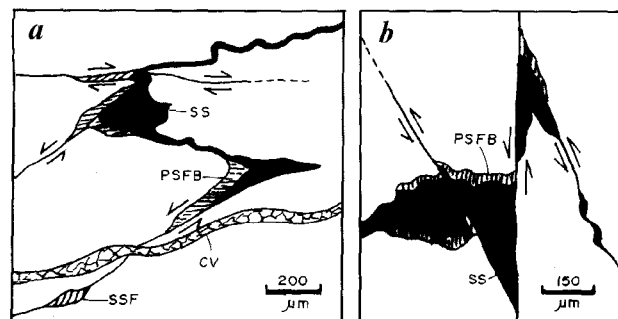


Figure 8. *a*, Sketch from photomicrograph showing the relation between stylolite seam, shear fracture and fibrous band. Shear fractures extending from the margin of the stylolite seam into the hosting limestone displace the fibrous bands associated with the stylolite seam. Late blocky calcite vein (CV) cuts across the shear fractures. Note the attenuated and folded nature of the stylolite limbs. Limestone host is blank. PSFB, Pre-shearing fibrous band; SS, Stylolite seam; SSF, Syn-shearing fibrous band; *b*, Part of stylolite cone showing the time-relation of the two sets of shear fractures. Note that both the sets displace the stylolite seam (black), but one set is younger than the other. Limestone host is blank.

sedimentary pile, and additionally, in some cases to the tectonic stress. The textural inhomogeneities considered in the model are the natural non-uniform distribution pattern and frequency of the insoluble mineral grains (opaque and clay) in the rock, and also the inhomoge-

neous porosity (pore-maxima and pore-minima) of the rock mass. The pressure solution kinetics depends to a large extent on the relative pressure solubility of the minerals constituting the rock¹¹, and on the nature of the grain contacts³. The fluids available during the diagenetic stage are either the *in situ* pore fluid or the extraneous fluid supplied by the flowing groundwater, or both.

The kinetic model of stylolite genesis proposed here is based on the microstructures of the studied stylolites at different stages of their formation, as described earlier. The initiation of stylolite takes place at the sites of microfractures or early joints, preferentially at those segments of the rock discontinuity elements that are oriented at a high angle to σ_1 (ref. 4). The initiation can also be at the bedding planes of the rock that contain textural heterogeneities, especially of uneven porosity and permeability distribution². The sites of microfractures and pore-maxima become locales of reduced pore-fluid pressure. Under these conditions, the unsaturated or poorly saturated fluids from outside flow into these low-pressure regions. The pore-fluid pressure re-equilibrates, and the fluids within the microfracture or highly porous bedding plane pressure-dissolve calcite and quartz of the rock. The microfracture or the bedding planes guide the fluid-flow in a direction perpendicular to or at a high angle to σ_1 . The actual fluid flow under local stress system in 3D is contained on surfaces parallel to the σ_2 - σ_3 plane, and is in a direction ideally parallel to σ_3 . The fluid flow creates a 'pressure solution wedge' (PSW) that is driven transverse to σ_1 through the rock mass along the initial microfracture or the bedding plane, thus facilitating its propagation. At the tip of the PSW the equant host-rock mineral grains develop pressure solution contacts (PSC) parallel to PSW ((2A), Figure 9a). These contacts suffer fluid-film diffusion, and in the presence of intergranular clay particles, these contacts become free-face pressure solution surfaces³. With continued grain-contact pressure-solution the grains are flattened, become inequant, and the PSCs approach one another⁶ to form a composite pressure-solution seam that helps propagate the PSW ((2B), (2C), Figure 9a).

As the original pressure-solution surface propagates, the residual insoluble mineral grains accumulate in the fluid pathways to form the stylolite seam that divides the rock into two blocks (X, Y, cf. (3), Figure 9a). The splitting of the rock mass into two rock-block partners is one of the prerequisites for stylolite differentiation. If the texture of these two rock-blocks is stable, meaning uniform to near-uniform distribution of the insoluble grains or the pores in them, the stylolite seam cannot differentiate because the pressure solution kinetics is uniform in both the rock-blocks. Since under this condition there is no instability at the stylolite walls, one block cannot differentially penetrate the other block at

any site to form the stylolite interdigitations. This results in smooth and planar stylolite seam or simply the pressure solution seam ((4), Figure 9a). On the other hand, and as is normally the case, if the rock texture and the mineral and pore distribution are not uniform in the two rock-blocks, the smoothness of the initial planar pressure-solution seam is lost, and the stylolite differentiation may take place. Two cases under this situation are considered.

In the first case, the two rock-block partners contain unevenly distributed pressure solution-resistant mineral grains (opaque and clay), and these grains may occur in clumps (RC, (1), Figure 9b) as in nature. As the two rock-blocks impinge on each other due to pressure solution of the intervening rock material and the solvent fluid escapes from the stylolite seam, the clumps reach the seam and block the transverse flow of the fluid. The fluid flow also gets impeded due to plugging and permeability loss of the stylolite seam by the accumulation of impervious and insoluble clay layers. This situation results in a polarity reversal of the fluid flow^{7,8}, which gets partitioned at the clump sites. A major part of the fluid starts to travel longitudinally in a direction nearly parallel to σ_1 at these sites on both sides of the stylolite plane, and the other part may flow transverse to σ_1 along the stylolite seam if permeability still persists in that direction ((2), Figure 9b). Since the opaque and especially the clay minerals increase the pressure solubility of the matrix minerals (calcite and quartz) in contact¹², these solution-resistant clumps move away from the stylolite plane parallel to the direction of σ_1 , forming stylolite cones at these sites. Figure 2 shows the stylolite microstructures that form by this mechanism at the initial stage of stylolite differentiation. As these clumps migrate away from the stylolite plane in response to increased pressure solution of the matrix minerals in contact with the clumps located on the cone apex, the cone head gathers more insoluble residue. This in turn enhances the pressure solution at the cone head and increases the head thickness as exemplified by the microstructures shown in Figure 4. This 'feedback' kinetics⁸ results in an increase in the thickness of the stylolite head that greatly augments the amplification process.

In the second case, the two participating rock-blocks are homogeneous in terms of insoluble mineral-grain distribution, but may contain textural instabilities imparted by non-uniform distribution of pore-maxima and pore-minima. The latter feature could either be an inherent rock character or the result of porosity amplification through the action of anisotropic stress². In regions of pore-maxima, local stress increases by focusing of the compressive stress⁸ that acts on larger free-grain surface area formed due to higher porosity. As a consequence, the pressure-solution increases at these sites creating more pore space. The pressure-solution mecha-

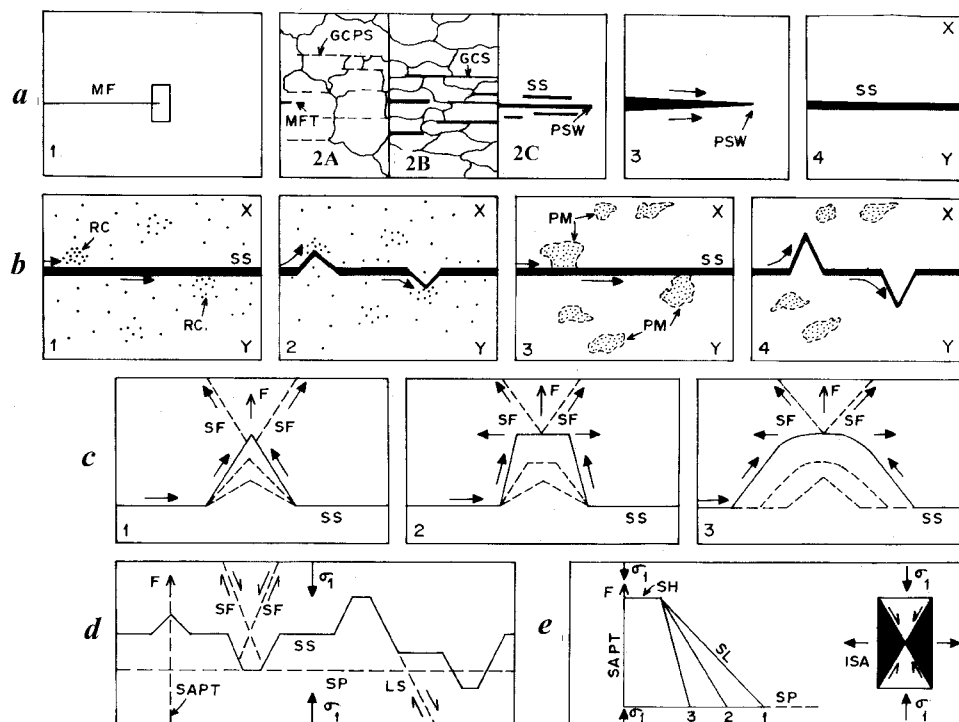


Figure 9. Kinetic model of differentiated stylolite genesis. **a**, Formation of planar and smooth stylolite seam from an initial microfracture (MF) within the rock-mass having no textural inhomogeneity and instability. The mechanism of microfracture propagation by grain boundary-controlled pressure solution within a block (rectangle) at the tip of MF in (1) is shown in (2A), (2B) and (2C). Small solid arrow, Pressure solution wedge and local fluid-flow direction; GCPS, Grain-contact pressure solution; GCS, Grain-contact seam; MFT, Microfracture tip; PSW, Pressure solution wedge; X, Y Two rock-blocks separated by stylolite seam; SS, Stylolite or pressure solution seam. **b**, Formation of conical stylolite geometry from planar and smooth stylolite seam due to textural inhomogeneity in the two rock-blocks (X, Y). Small solid arrow, Local fluid-flow direction; Dot, Opaque and clay mineral grains; PM, Pore-maxima; RC, Solution residue mineral clump; SS, Stylolite seam. **c**, Mechanism of stylolite amplification from an initial low-amplitude conical type (1) to columnar (2) and wavy (3) types by progressive displacement of the stylolite head away from the initial stylolite seam location in the direction of stylolite facing. Small solid arrow, Local fluid-flow direction; F, Stylolite facing; SF, Shear fracture; SS, Stylolite seam. **d**, Relation between stylolite elements and diagenetic stress system; F, Stylolite facing; LS, Limb-shear plane; SAPT, Stylolite axial plane trace; SF, Shear fracture; SP, Stylolite plane; SS, Stylolite seam. **e**, Relation between the orientation of stylolite head (SH), stylolite limb (SL) and stress system that controls stylolite microstructures. (Inset) Stress regime where the black areas are the instantaneous extension domains and the blank areas, instantaneous shortening domains. Lines 1, 2, 3 represent the orientation of limbs of a hypothetical stylolite at different stages of rotation from the initial position in the stretching field (1) to the shortening field (3) across the shear plane (2); F, Stylolite facing; ISA, Instantaneous stretching axis; SAPT, Stylolite axial plane trace; SP, Stylolite plane.

nism in such cases is thus self-accentuating. When these sites of high porosity reach the nearly plugged planar stylolite seam ((3), Figure 9b), much in the same manner as the solution-resistant mineral clumps do in the first case (discussed above), the transverse fluid-flow is perturbed at these sites. Much of the fluid flows away from the seam into these pore-maxima sites. Subsequent pressure solution and accumulation of residual minerals accentuate the instability and give rise to uneven and generally conical stylolite seam geometry ((4) Figure 9b).

In nature, however, both the above rock characters, considered for the two cases, coexist. Notably, in both the cases (e.g. controls of mineral clumps and pore-

maxima) the sites of textural instability dictate the location of the stylolite cones. Since the instability sites in the rock mass are randomly distributed in nature, the spacing and the geometry of the stylolite cones and columns in differentiated stylolites are also random.

With continued pressure solution and migration of the sites of instability away from the initial planar stylolite seam in a direction parallel to σ_1 , the stylolite amplitude or the height of the cone increases. This feature is exemplified in the microstructures shown in Figure 3. This mechanism controls the amplification of the stylolite cones (Figure 9c). At this stage of stylolite formation, the rock has been compacted to such an extent that shear fractures, generally in conjugate sets, can develop.

It has been experimentally shown that the permeability for the fluid flow along the shear surfaces is one order of magnitude higher than across such surfaces¹³. The microstructures indicate that these shear fractures are connected to the stylolites seams (Figure 5), and hence, these could act as the pathways for a part of the saturated fluid to escape the stylolites zones. The cylindrical and prismatic forms of the stylolites in 3D suggest that a part of the fluid may also flow parallel to the stylolite axis⁸ in the direction of σ_3 . Syntectonic quartz and calcite fibres may precipitate from this solvent fluid at dilatant sites within the shear fractures. That shearing plays an important role in stylolite genesis is evident from the geometry of asymmetric stylolites (slickolites)¹⁴, where the stylolite axial plane and the stylolite facing are not orthogonal to the stylolite plane. The latter plane in slickolite is generally a pre-existing fracture oblique to σ_1 along which subsequent shearing takes place, while the stylolite differentiates in the direction parallel to σ_1 (ref. 4). Clearly, the stylolite symmetry depends on the orientation of the initial pressure solution surface with respect to σ_1 .

Two situations may arise during the amplification of the stylolite cones. In the first situation the base of the cone (or base of the prism in 3D) does not increase in size, i.e. the ends of the cone-base/prism-base are anchored at the stylolite planar segments. As a result, during amplification the increase in the cone/prism height is accompanied with the steepening of the cone/prism sides ((1) Figure 9c). This steeply conical/prismatic type of stylolite is rather uncommon because as the cone/prism height increases with progressive pressure solution, the apex or the stylolite head also increases in thickness due to increased concentration of insoluble minerals, and tends to be flattened perpendicular to σ_1 . The head flattening is also aided by local transverse fluid-flow parallel to the stylolite plane in the apex region, causing lateral seam growth at the head region ((2) Figure 9c). The head migration in the direction of σ_1 simultaneously with the head flattening results in steep stylolite limbs that form the columnar stylolites. Since the fluid-flow is limited on the limbs due to their steepness, the seam thickness at the limbs is much smaller than that at the flat heads. In the second situation, the cone/prism base is enlarged during amplification, i.e. the ends of the cone/prism base are not anchored at the stylolite planar segments. In this case, the mechanism described for the first situation above forms the wavy stylolite (or cylindrical stylolite in 3D) ((3) Figure 9c).

The stylolite morphology indicates that the late-or post-diagenetic stage is marked by shear-related microstructures. Clearly, the shearing is caused by the resolved non-coaxial strain in the partially compact rock mass and by strain partitioning at the inclined stylolite limbs. It is related to the local stress system,

linked either to compaction or tectonic stress or to both. The kinematic relationship between the different components of this stress system and the stylolite geometry in 2D is shown in Figure 9d. The stylolite axial plane trace (SAPT) is the obtuse bisetrix of the dihedral angle of the conjugate shear planes, while the stylolite facing (F) normal to the stylolite plane (SP), gives the local σ_1 axis. The SP trace is parallel to σ_2 . The modification of the stylolite geometry, and particularly the nature and internal fabrics of their heads and limbs, depend on the position of these elements with respect to the local and instantaneous strain regime. The stylolite heads that are orthogonal to σ_1 are flattened and those at a low-to-moderate angle to σ_1 show kink-bands on the internal layering (Figure 4). The limbs are inclined to σ_1 at variable angles, and those lying in the instantaneous stretching field (limb 1, Figure 9e) are attenuated and boudinaged. Similarly, the steep limbs lying in the instantaneous shortening field (limb 3, Figure 9e) are buckled, while the limbs parallel to the shear planes (limb 2, Figure 9e) show layer-parallel shearing (limb-shear), and contain S-C type non-coaxial strain fabric. Any given stylolite limb and head segments may rotate under progressive local strain and pass through different instantaneous strain regimes, and show the corresponding microstructural features.

The kinetics of fibrous band formation and the growth of calcite and quartz fibres in them at the stylolite seam margins (Figure 3) has been discussed elsewhere¹⁰, and is not considered in the stylolite genesis model enumerated above. The geometry of the fibrous bands indicates that these may grow during the late phase of stylolite differentiation. The initial fibre growth may be 'crack-seal'-type¹⁵, but the dominant late growth is antitaxial, simulating Taber-growth conditions¹⁶. The fibre-growth kinetics is controlled by the asperity of the stylolite seam walls on which the fibres grow, such that the asperities act as fibre grain-boundary attractors¹⁷. The preferred dimensional orientation of the mineral fibres parallel to the stylolite axial plane trace or to σ_1 , irrespective of the stylolite seam orientation, is capable of tracking the opening trajectory of the dilation zones containing the fibrous bands. This indicates displacement-controlled fibre growth at the dilation zones formed on the stylolite walls that shrink and collapse inward due to volume loss of the stylolite seam material at the late diagenetic stage of stylolite formation.

The main conclusion from this study is that the variation in the stylolite geometry and microstructures is a function of the rock heterogeneity and textural instabilities. The instability is the result of non-uniform distribution and variable frequency in the rock mass of such controlling textural elements as pressure-insoluble mineral grains of different sizes, high and low porosity and permeability sites, etc. Pressure-solution kinetics is self-

accentuating, and hence the stylolite genesis that depends on pressure solution is a progressive phenomenon, the geometric response of which is its differentiation. The kinetics of differentiated stylolite formation is driven by diagenetic compressive stress and/or tectonic deformation stress and their locally resolved shear components, and is also controlled by the perturbations of solvent fluid-flow at sites of textural instabilities.

1. Manten, A. A., *Geol. Mijnbouw*, 1966, **45**, 269–274.
2. Merino, E., Ortoleva, P. and Strickholm, P., *Contrib. Mineral. Petrol.*, 1983, **82**, 360–370.
3. Renard, F., Park, A., Ortoleva, P. and Gratier, J.-P., *Tectonophysics*, 1999, **312**, 97–115.
4. Peacock, D. C. P., *J. Struct. Geol.*, 2001, **23**, 329–341.
5. Fletcher, R. C. and Pollard, D. D., *Geology*, 1981, **9**, 419–424.
6. Trurnit, P., in *Recent Development in Carbonate Sedimentology in Central Europe* (eds Miller, G. and Friedman, G. M.), Springer Verlag, Berlin, 1968, pp. 76–84.
7. Guzzetta, G., *Tectonophysics*, 1984, **102**, 383–394.
8. Bayly, B., *J. Geol.*, 1986, **94**, 431–435.

9. Sinha-Roy, S., *J. Geol. Soc. India* (in press, a).
10. Sinha-Roy, S., *ibid* (in press, b).
11. Heald, M. T., *J. Geol.*, 1955, **63**, 101–114.
12. Bos, B., Peach, C. S. and Spiers, C. J., *Tectonophysics*, 2000, **327**, 173–194.
13. Zhang, S. and Cox, S. F., *J. Struct. Geol.*, 2000, **22**, 1385–1393.
14. Ramsay, J. G. and Huber, M. I., *The Techniques of Modern Structural Geology: Folds and Fractures*, Academic Press, London, 1987, p. 480.
15. Ramsay, J. G., *Nature*, 1980, **284**, 135–139.
16. Means, W.D. and Li, T., *J. Struct. Geol.*, 2001, **23**, 857–863.
17. Hilgers, C., Koehn, D., Bons, P. D. and Urai, J. L., *ibid*, 2001, **23**, 873–885.

ACKNOWLEDGEMENTS. This work is part of a project financially supported by the Department of Science and Technology, Govt. of India, New Delhi. I thank Dr P. Ghosh, Executive Director, Birla Institute of Scientific Research, Jaipur, for the facilities provided.

Received 27 August 2001; revised accepted 15 January 2002